



Scholars Research Library
(<http://scholarsresearchlibrary.com/archive.html>)



ISSN : 2231- 3176
CODEN (USA): JCMMDA

QSPR studies on the behavior of 2-Thiomethylbenzimidazole (TMBI) during Copper corrosion inhibition efficiency in 1M HNO₃

Ehouman Ahissan Donatien, Niamien Paulin Marius*, Diaby Sékou and Trokourey Albert

Laboratoire de Chimie Physique, Abidjan, Université Félix Houphouët Boigny, Abidjan-Cocody, Côte d'Ivoire

ABSTRACT

A theoretical study of the behaviour of 2-Thiomethylbenzimidazole (TMBI) against copper corrosion in 1M HNO₃ has been performed. This molecule was recently used as corrosion inhibitor. It was found that when the molecule adsorbed on the copper surface, the molecular structure influences the interaction mechanism and by extension the inhibition efficiency. DFT calculations have been used to optimize the geometry of TMBI and to determine the quantum chemical descriptors parameters relevant to its potential action as corrosion inhibitor. Furthermore, equations linking corrosion efficiency and some sets of molecular structure parameters were proposed using the non linear model of Lukovits. The theoretical results were found to be consistent with the experimental data reported.

Keywords: copper corrosion inhibition, nitric acid, DFT calculations, geometry optimization, molecular and reactivity parameters, corrosion inhibition efficiency.

INTRODUCTION

The study of corrosion processes and their inhibition by organic compounds [1-3] is a very active field of research. Several organic compounds are effective inhibitors of acid corrosion of a number of metals and alloys. Recently [4, 5], the effectiveness of an inhibitor molecule has been related to its spatial as well as electronic structure.

Quantum chemical methods [6] have already proven to be very useful in determining the molecular structure as well as elucidating the electronic structure and reactivity. Density functional theory (DFT) [7] has become the dominant tool in chemistry and physics for calculations of electronic structure. Through the development [8] of accurate approximations to the exchange-correlation energy functional, the Kohn-Sham method [9] has been extensively and successfully applied to the study of simple and complex chemical systems. Density functional theory (DFT) [10-13] has provided a very useful framework for developing new criteria for rationalizing, predicting and eventually understanding many aspects of chemical processes.

DFT has also provided a very solid framework for the study of chemical reactivity. Through this approach, it has been possible to derive new fundamental variables of DFT chemically meaningful concepts that had been established intuitively [14] like the electronegativity (χ), the global hardness (η) and furthermore the fraction of electrons transferred (ΔN).

Quantitative Structure Property Relationship (QSPR) [15-19] has been derived for various set of corrosion inhibitors, as attempts to find consistent relationship between the variations in the values of molecular properties and the inhibitor activity for series of compounds. Two different approaches [20, 21] including empirical method and semi-empirical method have been used in the development of QSPR for corrosion inhibitors. Attempts [22-24] have been made to predict corrosion inhibition efficiency with some sets of quantum descriptors including: E_{HOMO} , energy

of the highest occupied molecular orbital, E_{LUMO} , energy of the lowest unoccupied molecular orbital, dipole moment (μ) and energy gap ($E_{\text{LUMO}}-E_{\text{HOMO}}$).

The low computational cost, combined with useful accuracy [25], has made DFT a standard technique in most branches of chemistry and materials science. Electronic structure problems in variety of fields are currently being tackled. Generalized gradient approximations (GGA) [26] produced accuracy, useful for chemical calculations. However, the GGA's approach [27] is not always sufficient for a correct description of the chemical properties of organic molecules. One degree of additional precision [27] is reached by using hybrid exchange-correlation functional. The tested DFT methods include three hybrid functionals B3LYP [28, 29], B3PW91 [30] and PBE1PBE [31]. The survey of theoretical corrosion literature presented by Gece [32] demonstrates that quantum chemistry is a powerful tool to study the fundamental, molecular-level processes related to corrosion inhibition.

The aim of the present work is to find the best tested set of structural and reactivity parameters which leads to the inhibition efficiency of 2-Thiomethyl-benzimidazole (TMBI) against copper corrosion in 1M HNO_3 , using the best tested exchange-correlation functional in conjunction with the best tested basis set in DFT calculation.

MATERIALS AND METHODS

Computational details

In computational chemistry tools, DFT offers the fundamentals for interpreting multiple chemical concepts used in different branches of chemistry. In order to explore the theoretical-experimental consistency, quantum calculations were performed with complete geometry optimization using standard Gaussian 03 W software package [33]. Geometry optimization were carried out at DFT level by respectively B3LYP, B3PW91 and PBE1PBE functionals in conjunction with four basis sets including: 6-31G (d, p), 6-31+G (d, p), 6-31++G (d, p) and 6-311G (d, p). All theoretical calculations were determined in gas phase and in the approximation of the isolated molecule. The molecular structure of TMBI is presented in Figure 1.

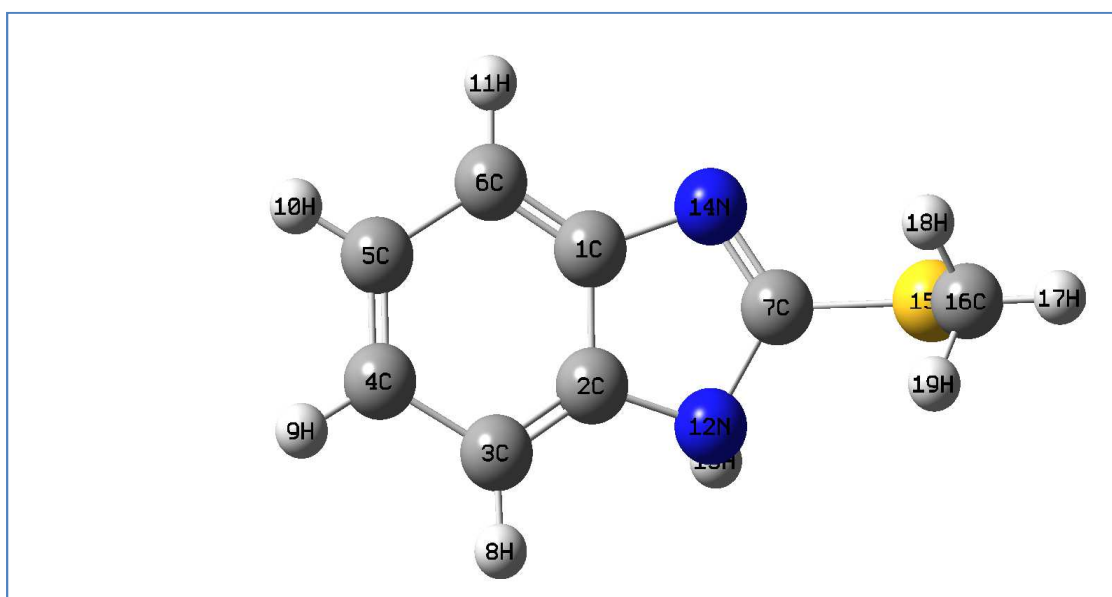


Figure1. Molecular structure of 2- Thiomethylbenzimidazole (TMBI)

RESULTS AND DISCUSSION

Geometric parameters

Some calculated geometry parameters of TMBI, obtained with B3LYP, B3PW91 and PBE1PBE with the basis sets: 6-31G (d, p), 6-31+G (d, p), 6-31++G (d, p) and 6-311G (d, p) were compared with experimental values [34] reported for geometrical parameters derived from X-ray crystal structure.

As observed in Tables 1 (A, B, C, D) the corresponding geometrical parameters obtained have similar values. All tested methods showed good results for bond lengths and bond angles when compared with the reported X-ray data. At this point, it was difficult to define which method is more appropriate to use for the studied compound.

Table1A. Calculated geometries with 6-31G (d, p) (Bond length in Å and bond angle in degree)

Parameters (Å, °)	B3LYP	B3PW91	PBE1PBE	Experimental values [34]
C1-C4	1.415	1.413	1.411	1.397
C7-N14	1.309	1.308	1.306	1.308
C7-N12	1.380	1.375	1.372	1.359
C7-S15	1.764	1.755	1.751	1.755
C7-S15-C16	99.07	98.98	98.69	98.78
C7-N12-H13	126.26	126.25	126.22	126.10

Table1B. Calculated geometries with 6-31+G (d, p) (Bond length in Å and bond angle in degree)

Parameters (Å, °)	B3LYP	B3PW91	PBE1PBE	Experimental values [34]
C1-C4	1.415	1.413	1.411	1.397
C7-N14	1.311	1.309	1.307	1.308
C7-N12	1.381	1.376	1.373	1.359
C7-S15	1.762	1.753	1.749	1.755
C7-S15-C16	99.55	99.35	99.08	98.78
C7-N12-H13	126.20	126.20	126.18	126.10

Table 1C. Calculated geometries with 6-31G ++ (d, p) (Bond length in Å and bond angle in degree)

Parameters (Å, °)	B3LYP	B3PW91	PBE1PBE	Experimental values [34]
C1-C4	1.416	1.413	1.411	1.397
C7-N14	1.311	1.309	1.307	1.308
C7-N12	1.381	1.376	1.373	1.359
C7-S15	1.762	1.753	1.749	1.755
C7-S15-C16	99.54	98.35	98.08	98.78
C7-N12-H13	126.26	126.20	126.18	126.10

Table1D. Calculated geometries with 6-311G (d, p) (Bond length in Å and bond angle in degree)

Parameters (Å, °)	B3LYP	B3PW91	PBE1PBE	Experimental values [34]
C1-C4	1.413	1.411	1.409	1.397
C7-N14	1.306	1.305	1.303	1.308
C7-N12	1.379	1.374	1.370	1.359
C7-S15	1.763	1.753	1.749	1.755
C7-S15-C16	99.13	98.02	98.76	98.78
C7-N12-H13	126.34	126.33	126.29	126.10

Total ground-state energy of TMBI

The total ground-state energy of TMBI in function of the basis set has been represented in figure 2. As it can be observed, the lowest values of the ground-state energy are obtained with the hybrid functional B3LYP for all tested basis sets.

The highest values of the ground-state energy are obtained with the hybrid functional PBE1PBE for all tested basis sets. The ground-state energy values are then in a descent order as: PBE1PBE > B3PW91 > B3LYP.

The variational principle states that the ground-state energy is given by:

$$E = \min_n \left[F[n] + \int d^3r V_{ext}(r)n(r) \right]$$

Where $F[n]$, $V_{ext}(r)$ and $n(r)$ are respectively a universal functional, the external potential and the electronic density.

Considering this principle, one can see that B3LYP/6-311G (d, p) seems to be the more appropriate method for the calculations of the structural and reactivity parameters.

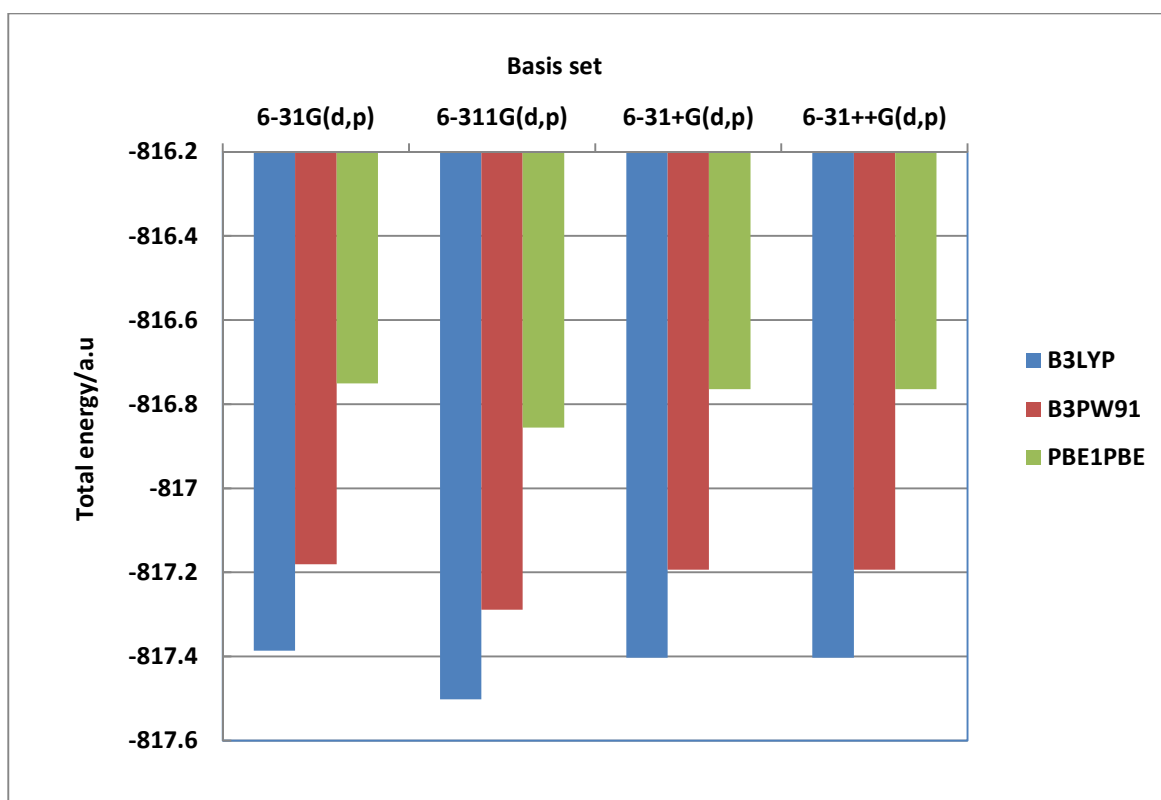


Figure 2. Ground-state energy for the studied basis sets

Molecular and reactivity parameters

The calculations of the molecular parameters were carried out. The following quantum chemical parameters were considered: energy of highest occupied molecular orbital (E_{HOMO}), energy of the lowest unoccupied molecular orbital (E_{LUMO}), the energy gap ($E_{LUMO}-E_{HOMO}$) and the dipole moment μ . All the above mentioned parameters are given in Tables 2.

Table 2. Structural and reactivity parameters of the studied compound

Method	E_{LUMO}/eV	E_{HOMO}/eV	χ/eV	η/eV	ΔN	δ_{NS}/e	μ (D)
6-31G (d, p)	-0.268	-5.635	2.951	2.683	0.378	-1.204	1.718
6-31+G (d, p)	-0.671	-5.899	3.285	2.614	0.324	-1.207	1.786
B3LYP/ 6-31++G (d, p)	-0.671	-5.899	3.285	2.614	0.324	-1.306	1.851
6-311G (d, p)	-0.556	-5.856	3.206	2.650	0.335	-1.202	1.786
6-31G (d, p)	-0.335	-5.729	3.042	2.657	0.361	-1.198	1.733
6-31+G (d, p)	-0.671	-5.930	3.300	2.629	0.319	-1.198	1.854
B3PW91/ 6-31++G (d, p)	-0.671	-5.929	3.300	2.629	0.319	-1.186	1.848
6-311G (d, p)	-0.593	-5.905	3.249	2.656	0.326	-1.202	1.820
6-31G (d, p)	-0.136	-5.884	3.010	2.874	0.343	-1.204	1.725
6-31+G (d, p)	-0.479	-6.090	3.284	2.805	0.302	-1.203	1.844
PBE1PBE/ 6-31++G (d, p)	-0.479	-6.089	3.284	2.805	0.302	-1.203	1.839
6-311G (d, p)	-0.371	-6.052	3.211	2.840	0.311	-1.209	1.799

According to DFT-Koopman's Theorem [35-37], the ionization potential, I can be approximated as the negative of the highest occupied molecular orbital (HOMO) energy:

$$I = -E_{HOMO}$$

The negative of the lowest unoccupied molecular orbital (LUMO) energy is similarly related to the electron affinity A :

$$A = -E_{LUMO}$$

The global electronegativity, χ , which is identified in the finite difference approximation as the negative of the chemical potential is given by:

$$\chi = -\mu = \frac{I + A}{2}$$

The global hardness η is defined as:

$$\eta = \frac{I - A}{2}$$

During the interactions of TMBI with the copper surface, electrons flow from the lower electronegativity of TMBI to the higher electronegativity of copper surface until the chemical potential becomes equalized. The fraction of the transferred electrons, ΔN , was estimated according to Pearson [38]:

$$\Delta N = \frac{\chi_m - \chi_i}{2(\eta_m - \eta_i)}$$

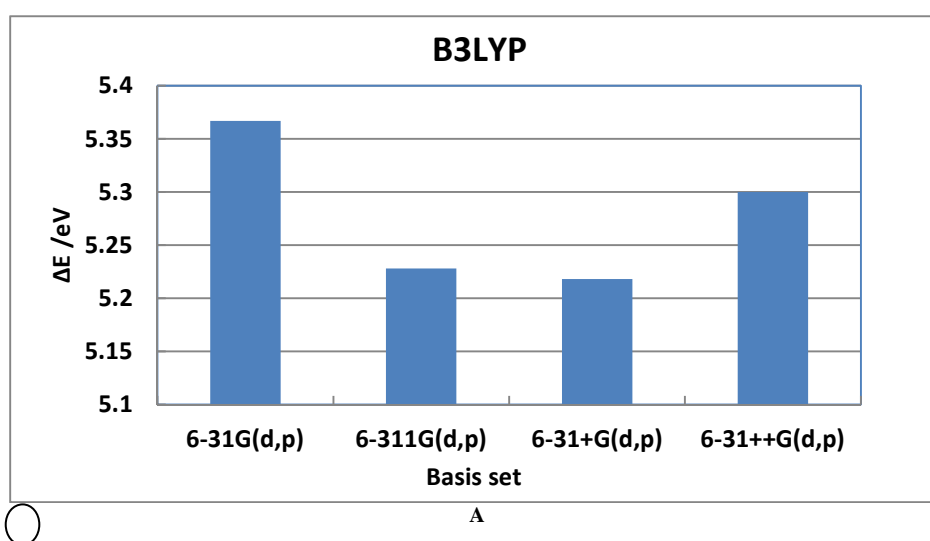
Where the indices m and i refer to copper and the inhibitor respectively. The calculation of ΔN was carried out, using a theoretical value of 4.98 eV/mol according to Pearson electronegativity scale [39] and η value of 0 eV/mol for copper atom [40].

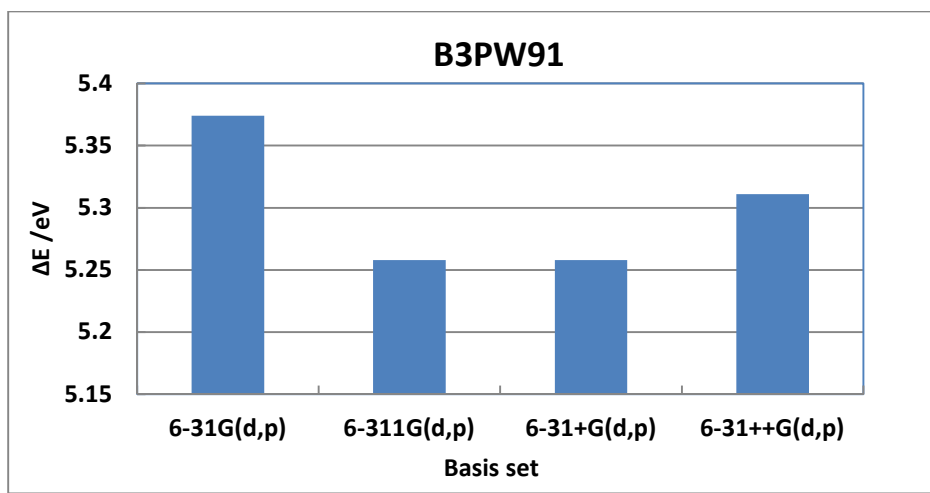
Figure 3 represents the energy gap in function of the basis set. The energy gap is related to the corrosion inhibition efficiency: the lowest LUMO-HOMO energy gap is correlated with the highest corrosion inhibition efficiency. Referring to Figure 3, one can range the values of the energy gap in the descent order: 6-31G (d, p) > 6-31++ G (d, p) > 6-311 G (d, p) > 6-31+ G (d, p). At this point, only 6-311 G (d, p) and 6-31+ G (d, p) can be chosen to model corrosion efficiency since TMBI has proven to be good corrosion inhibitor [41, 43].

In order to choose the best method, we have also examined ΔN whose values correlate strongly with experimental inhibition efficiencies [42]. The highest value of ΔN will favor higher inhibition efficiency. At this stage, the best method could be B3LYP/6-311G (d, p).

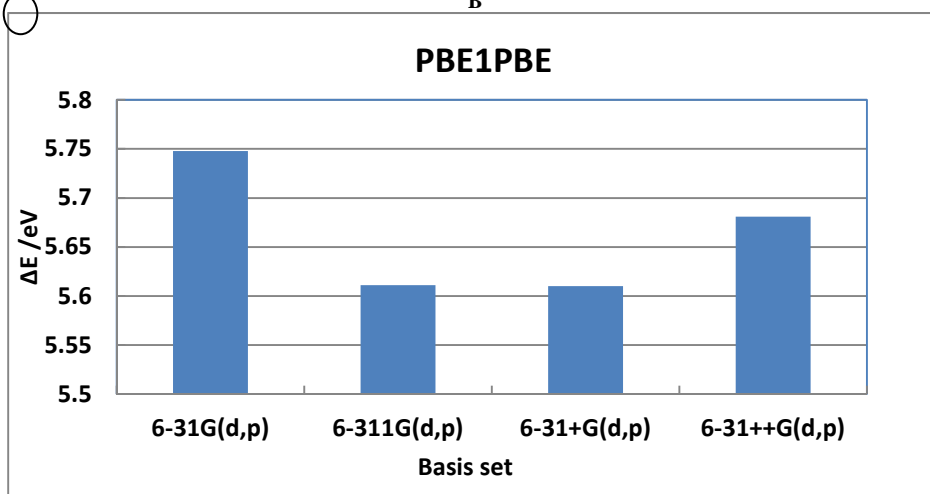
Another parameter that can be taken into account when choosing the method for molecular properties calculations is CPU time (or process time) which is the amount of time for which a central processing unit (CPU) is used for processing instructions of a computer program. Figure 4 shows the representation of CPU time in function of the basis set for each studied hybrid functional.

Observing figure 4, one can see that the lowest value of CPU time corresponds to 6-31G (d, p) and the highest value is related to 6-31G++ (d, p). Unfortunately, 6-31G (d, p) cannot be chosen because it has not the lowest value of total energy. From this point of view, only 6-311G (d, p) and 6-31+G (d, p) should be considered. The CPU time value's of 6-311 G (d, p) is lower than that of 6-31+ G (d, p). So only 6-311G (d, p) could be chosen. Considering all the above statements, it seems evident that the more appropriate method for TMBI's properties calculations is B3LYP/6-311G (d, p).



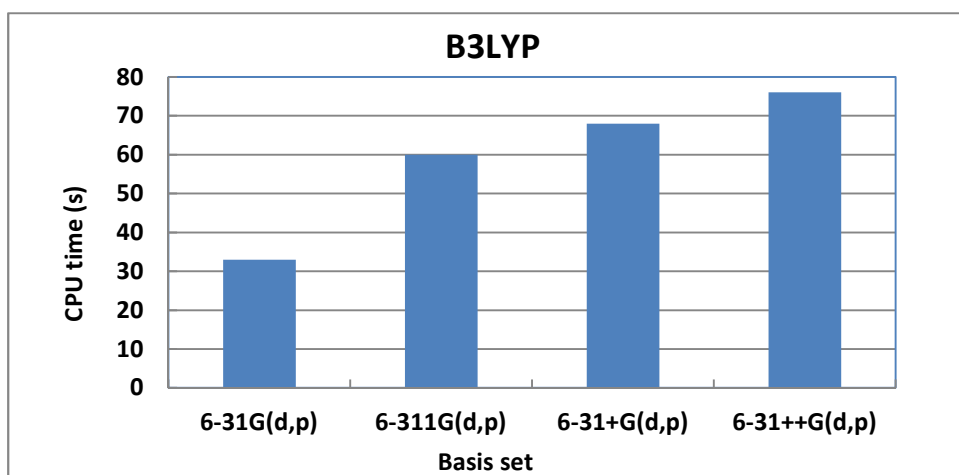


B



C

Figure 3: Energy gap in function of basis set



A

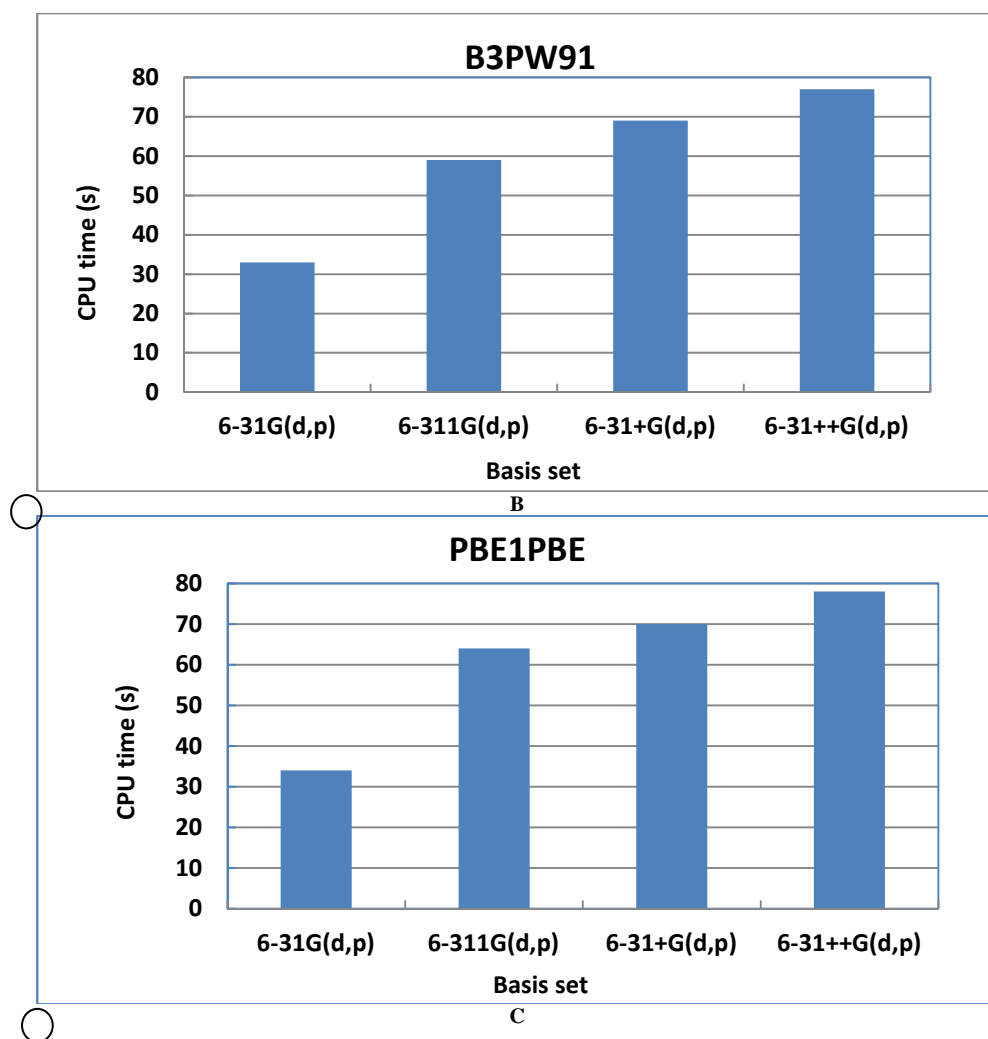


Figure 4: CPU time in function of basis set

Corrosion inhibition efficiency modeling

The inhibition efficiency of an organic molecule against corrosion depends essentially [44, 45] on the properties/descriptors parameters of that molecule including: HOMO energy, LUMO energy, LUMO-HOMO energy gap, dipole moment, fraction of electrons transferred, etc. Other parameters [46] routinely used as variables in molecular properties modeling procedures are partial atomic charges.

QSPR, quantitative structure–property relationships, are mathematical models that attempt to relate the structure-derived features of a compound to its biological or physicochemical activity. Similarly, quantitative structure–toxicity relationship (QSTR) or quantitative structure–pharmacokinetic relationship (QSPkR) is used when the modeling applies on toxicological or pharmacokinetic systems. The chemical structure is represented at molecular level by some sets of descriptors that can be mathematically connected to experimental properties by QSPR model. So, such model generally will have the following form:

$$y = a_0 + a_1x_1 + a_2x_2 + \dots + a_nx_n$$

In this equation, y is the property, that is the dependent variable, x_1 to x_n represent the specific descriptor, while a_1 to a_n the coefficient of those descriptors; a_0 is the intercept of this equation.

In this work, attempts are made to correlate some sets of composite index (quantum chemical and reactivity parameters) with the experimental corrosion inhibition efficiency of the studied molecule. The non linear model (LKP) proposed by Lukovits *et al.* [47] for the study of the interactions of corrosion inhibitors with metals surface in acidic medium is used; its derivation was based on the Langmuir adsorption isotherm to give the following relationship:

$$IE_{calc}(\%) = \frac{(Ax_j + B)C_i}{1 + (Ax_j + B)C_i} * 100$$

Where **A** and **B** are real constants determined by solving the system of simultaneous equations obtained with the different values of the inhibitor concentration C_i . A quantum or a reactivity parameter is represented by x_j . In this work, taking the number of concentrations (four concentrations) into account, we have considered several sets of three quantum chemical or reactivity parameters (x_1, x_2, x_3). The obtained equation has the following form:

$$IE_{calc}(\%) = \frac{(Ax_1 + Bx_2 + Dx_3 + E)C_i}{1 + (Ax_1 + Bx_2 + Dx_3 + E)C_i} * 100$$

We obtained a system of four equations with four unknowns. The calculations have been performed using EXCEL software. The calculated values of **A**, **B**, **D** and **E** for the different sets of parameters and for concentrations range of 50 μ M to 1000 μ M are listed in Table 3.

Table 3. Values of A, B, D and E for different sets of three quantum chemical or reactivity parameters

Set of parameters	A	B	D	E
($\Delta E, \mu, \Delta N$)	19.948	16.577	-9.646	-132.094
($\Delta E, \mu, \delta_{NS}$)	7.768	16.373	11.179	-56.967
(E_{HOMO}, E_{LUMO}, μ)	0.044	0.687	0.418	-0.103
($E_{HOMO}, E_{LUMO}, \delta_{NS}$)	0.113	-0.061	-0.383	0.178
($E_{HOMO}, E_{LUMO}, \Delta N$)	-0.040	0.174	0.131	-0.172
($E_{HOMO}, \mu, \Delta N$)	0.016	-0.022	0.151	0.092
($E_{HOMO}, \mu, \delta_{NS}$)	0.326	0.812	-1.946	-1.874
($E_{LUMO}, \mu, \Delta N$)	-0.409	-0.284	0.241	0.207
($E_{LUMO}, \mu, \delta_{NS}$)	-0.113	18.349	17.792	-11.441

δ_{NS} is the sum of partial charges on nitrogen and sulfur atoms. The experimental inhibition efficiency data have been obtained by gravimetric method as described in our previous works [42, 43]. Those data are listed in Table 4.

Table 4. Inhibition efficiency for different concentrations at T = 25°C.

Concentration (C/M)	0	$5 \cdot 10^{-5}$	10^{-4}	$5 \cdot 10^{-4}$	10^{-3}
Corrosion rate ($\text{g cm}^{-2} \text{h}^{-1}$)	0.1085	0.0796	0.0574	0.0221	0.0122
IE (%) _{experimental}	-	26.68	39.02	79.67	88.78

The estimated efficiencies versus the experimental ones are shown in figures 5 A-I.

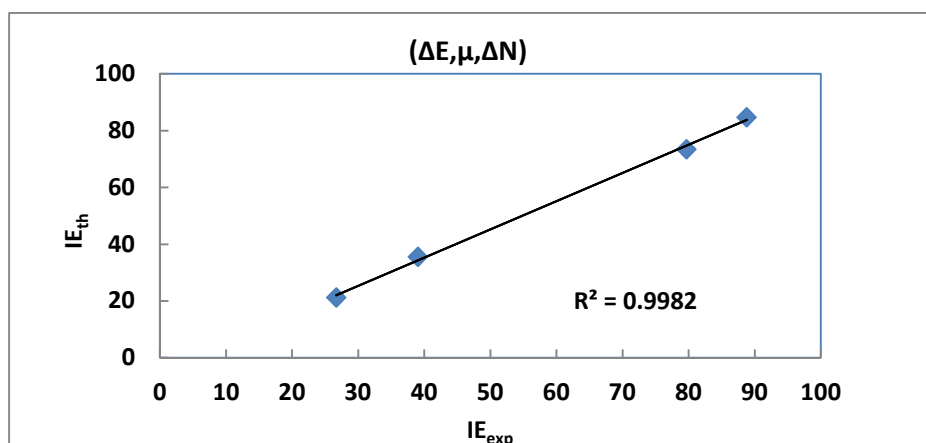


Figure 5 A. Theoretical vs. experimental efficiencies of TMBI for ($\Delta E, \mu, \Delta N$)

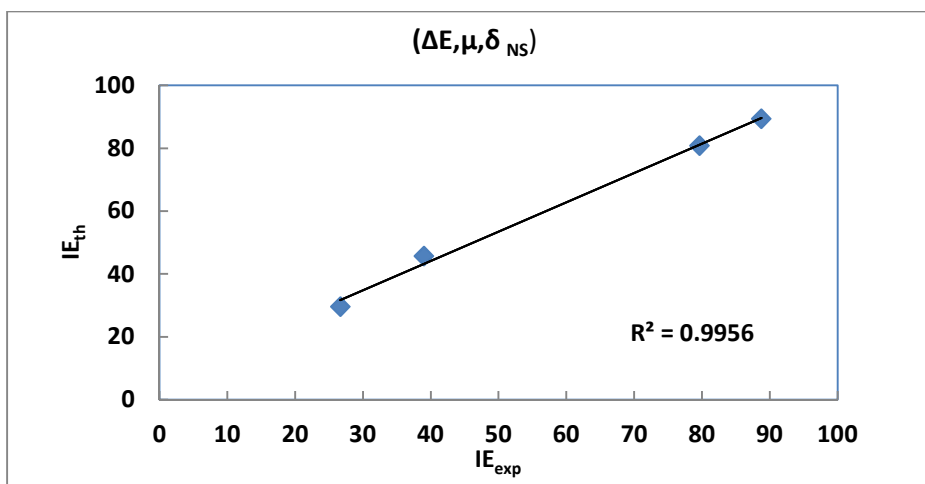


Figure 5 B. Theoretical vs. experimental efficiencies of TMBI for $(\Delta E, \mu, \delta_{NS})$

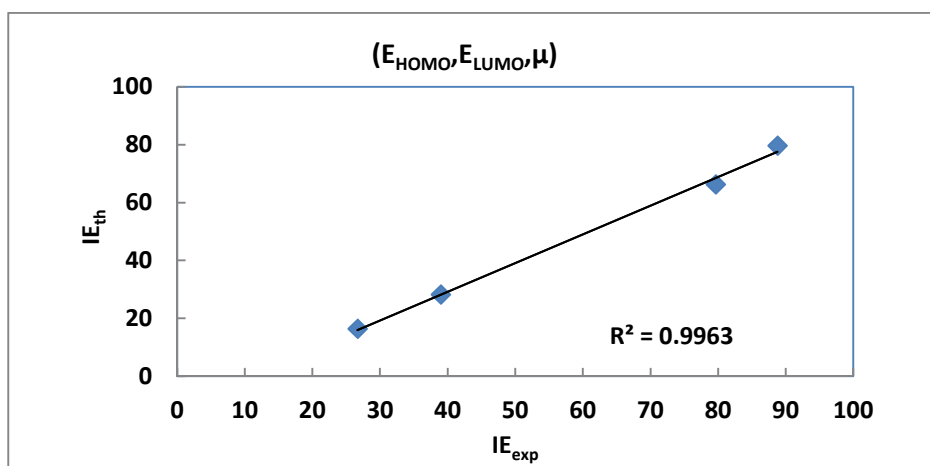


Figure 5 C. Theoretical vs. experimental efficiencies of TMBI for $(E_{HOMO}, E_{LUMO}, \mu)$

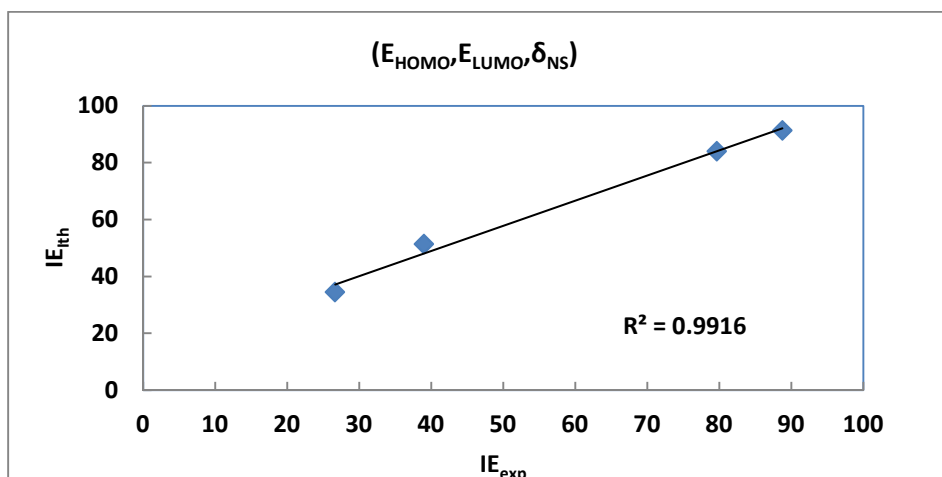


Figure 5 D. Theoretical vs. experimental efficiencies of TMBI for $(E_{HOMO}, E_{LUMO}, \delta_{NS})$

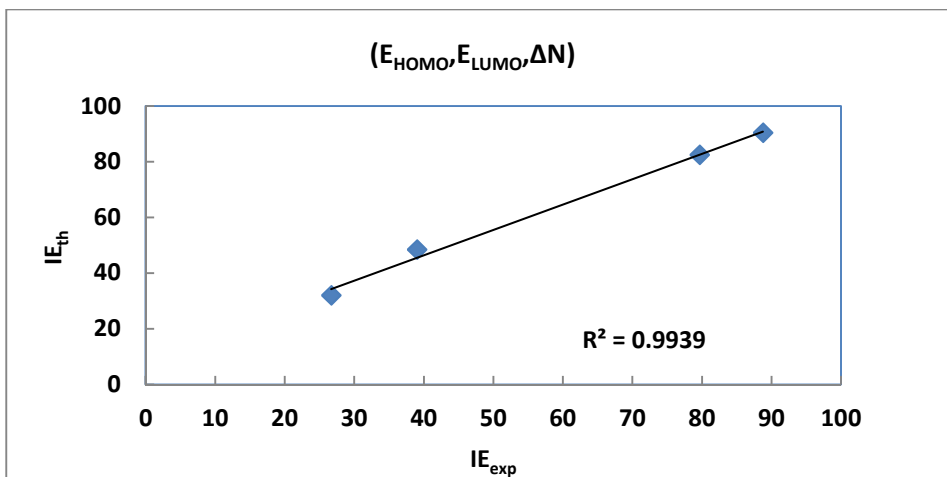


Figure 5 E. Theoretical vs. experimental efficiencies of TMBI for $(E_{HOMO}, E_{LUMO}, \Delta N)$

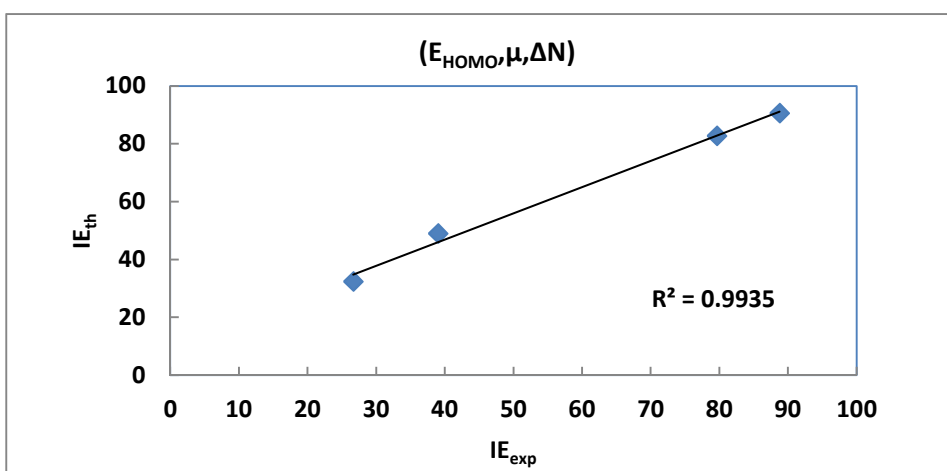


Figure 5 F. Theoretical vs. experimental efficiencies of TMBI for $(E_{HOMO}, \mu, \Delta N)$

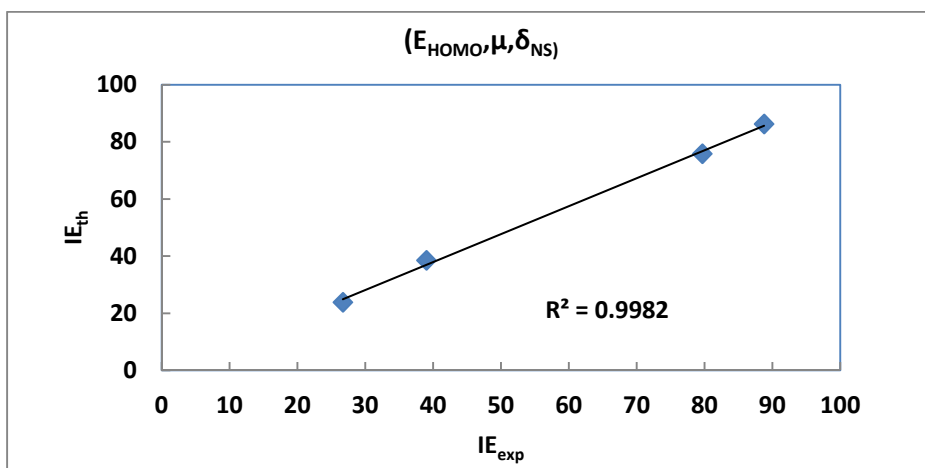
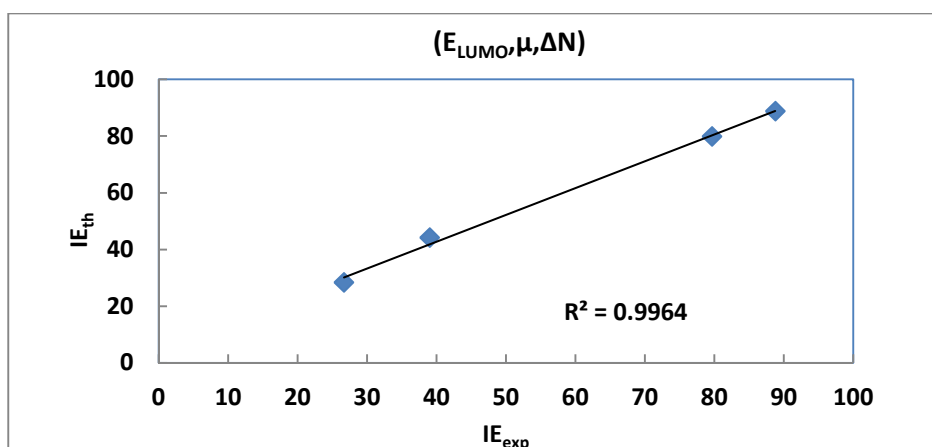
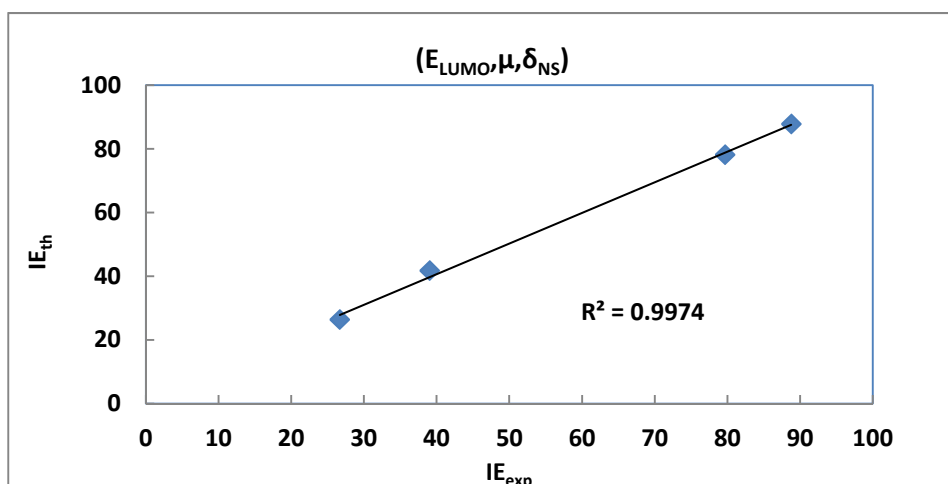


Figure 5 G. Theoretical vs. experimental efficiencies of TMBI for $(E_{HOMO}, \mu, \delta_{NS})$

Figure 5 H. Theoretical vs. experimental efficiencies of TMBI for $(E_{LUMO}, \mu, \Delta N)$ Figure 5 I. Theoretical vs. experimental efficiencies of TMBI for $(E_{LUMO}, \mu, \delta_{NS})$

Each studied set of molecular descriptors leads to an equation linking these parameters to the corrosion inhibition efficiency for a giving concentration in the inhibitor. All the obtained correlation coefficients from the representation of theoretical corrosion inhibition efficiencies versus experimental ones are nearly equal to unity. So, we have used statistical analysis, in order to determine the best set of parameters. These analysis are based on the sum of squared errors defined as:

$$SSE = \sum [IE(\%)_{theoretical} - IE(\%)_{estimated}]^2$$

The set of parameters $(E_{HOMO}, E_{LUMO}, \mu)$ which leads to a correlation coefficient value of $R^2=0.996$ and a value of SSE of 491.102 seems to be the worst descriptors set.

For the sets of parameters including: $(\Delta E, \mu, \Delta N)$, $(\Delta E, \mu, \delta_{NS})$, $(E_{HOMO}, E_{LUMO}, \delta_{NS})$, $(E_{HOMO}, E_{LUMO}, \Delta N)$, $(E_{HOMO}, \mu, \Delta N)$, $(E_{HOMO}, \mu, \delta_{NS})$ and $(E_{LUMO}, \mu, \Delta N)$ the obtained values of correlation coefficients are respectively $R^2 = 0,998$; $R^2 = 0,996$; $R^2 = 0,992$; $R^2 = 0,994$; $R^2 = 0,993$; $R^2 = 0,998$ and $R^2 = 0,996$. The values of the sum of squared errors are respectively 98.19; 54.39; 239.722; 125.69; 144.60; 29.54 and 29.44. Though the correlation coefficients are satisfying, the sum of squared errors are high.

The best set of parameters seem to be $(E_{LUMO}, \mu, \delta_{NS})$ for which the correlation coefficient value is 0.997 and that of the sum of squared errors 10.75.

CONCLUSION

These studies show that hybrid functional (B3LYP, B3PW91 and PBE1PBE) associated with the basis sets namely 6-31G (d, p), 6-31+G (d, p), 6-31++G (d, p) and 6-311G (d, p) lead to accurate values of bond length and bond angles. The B3LYP (Becke 3 parameters Lee, Yang and Parr) exchange correlation functional with 6-311G (d, p)

basis set is the optimal method for studying the inhibition efficiency of TMBI molecule in HNO₃ 1M. These studies also reveal that the best set of parameters for modeling the inhibition efficiency of TMBI molecule in the studied solution is ($E_{LUMO}, \mu, \delta_{NS}$). Strong correlations exist between the inhibition efficiency of the molecule and the studied sets of quantum or reactive parameters.

CONFLICT OF INTEREST

The authors declare that there is no conflict of interests regarding the publication of this paper. Also, they declare that this paper or part of it has not been published elsewhere.

CONTRIBUTION OF THE AUTHORS

This work was carried out in collaboration between all authors. Author NPM designed the study, performed the statistical analysis, computed the molecular descriptors and wrote the first draft of the manuscript. Author EAD monitored data collection tools, wrote the statistical analysis plan and revised the paper. Author DS managed the literature searches and revised the paper. Author TA analysed the data, drafted and revised the paper. All authors read and approved the final manuscript.

REFERENCES

- [1] G TrabANELLI, Corrosion Inhibitors in Corrosion Mechanisms, Marcel Dekkers Inc., **1987**, New York.
- [2] AY Musa, RT T Jalgham, AB Mohamad, *Corrosion Science* **2012**, 56,176.
- [3] SE Nataraja, T V Venkatesha, HC Tandon, *Corrosion Science* **2012**,60, 214.
- [4] AE Stoyanova, SD Peyerimhoff, *Electrochim. Acta* **2002**, 47, 1365.
- [5] LMR Valdez, AM Villafane, DG Maitnik, *J. Mol. Struct. (THEOCHEM)* **2005**,716, 61.
- [6] E Kraka, D Cremer, *J. Am. Soc.* **2000**, 122, 8245.
- [7] RM Dreizler, E K U Gross, Density functional theory, *Springer-Verlag*, **1990**, Berlin.
- [8] JP Perdew, S Kurth, Density Functionals for Non relativistic Coulomb systems in the New Century, *Springer*, **2003**, Berlin
- [9] W Koch, M C Holthausen, A Chemist's Guide to Density Functional Theory, **2001**, Wiley, New York.
- [10] P Hohenberg, W Kohn, *Phys. Rev.* **1964** B136, 864.
- [11] R G Parr, W Yang, Density functional theory of Atoms and Molecules, *Oxford University Press*, **1989**, New York.
- [12] R G Parr, W Yang, *J Am. Soc.* **1984**, 106, 4049.
- [13] M K Awad, *J. Electroanal. Chem.*, **2004**, 567,219.
- [14] R T Sanderson, *J Am. Soc.* **1952**, 74, 272.
- [15] I Lukovits, E Kalman, F Zucchi, *Corrosion* **2001**, 57, 3.
- [16] G Bereket, E Hur, C Ogretir, *J. Mol. Struct. (THEOCHEM)* **2002**, 578, 79.
- [17] J Cruz, E Garcia-Ochoa, M Castro, *J. Electrochem. Soc.*, **2003**, 150, B26
- [18] N Khalil, *Electrochim. Acta* **2003**, 48, 2635.
- [19] K F Khaled, K Babic-Samardzija, N Hackerman, *J. Appl. Electrochem.*, **2004**, 34,697.
- [20] F Bentiss, M Traisnel, H Vezin, M Lagrenée, *Corrosion Science* **2003**, 45, 371.
- [21] N O Obi-Egbedi, I B Obot, M I El-khaiary, S A Umoren, E E Ebenso, *Int. J. Electrochem. Sci.* **2011**, 6, 5649.
- [22] J Fang, J Li, *J. Mol. Struct. (THEOCHEM)* **2002**, 593,179.
- [23] K Y Dileep, M A Quraishi, B Maiti, *Corrosion Science* **2012**, 55, 254.
- [24] P M Niamien, A Trokourey, D Sissouma, *International Journal of Research, in Chemistry and Environment* **2012**, 2, 204.
- [25] I J Casely, J M Ziller, M Fang, F Furche, W J Evans, *J. Am. Chem. Soc* **2011**, 133, 5244.
- [26] J P Perdew, *Phys Rev* **1986**, B33, 8822.
- [27] A D Becke, *J. Chem. Phys.* 1996, 104, 1040.
- [28] A D Becke, *J. Chem. Phys.* **1993**, 98, 5648.
- [29] P J Stenphens, F J Delvin, C F Chabalwski, M J Frisch, *J. Phys. Chem.* **1994**, 98, 11623.
- [30] C Adams, V J Barone, *Chem. Phys.* **1999**, 110, 6158.
- [31] A D Becke, *Phys. Rev.* **1988**, A.38, 3098.
- [32] G Gece, *Corrosion Science* **2008**, 11, 2981.
- [33] M J Frisch, G W Trucks, H B Schlegel, G E Scuseria, M A Robb, J R Cheeseman, J A Montgomery, Jr., T Vreven, K N Kudin, J C Burant, J M Millam, S S Iyengar, J Tomasi, V Barone, B Mennucci, M Cossi, G Scalmani, N Rega, G A Petersson, H Nakatsuji, M Hada, M Ehara, K Toyota, R Fukuda, J Hasegawa, M Ishida, T Nakajima, Y Honda, O Kitao, H Nakai, M Klene, X Li, J E Knox, H P Hratchian, J B Cross, C Adamo, J Jaramillo, R Gomperts, R E Stratmann, O Yazyev, A J Austin, R Cammi, C Pomelli, J W Ochterski, P Y Ayala, K Morokuma, G A Voth, P Salvador, J J Dannenberg, V G Zakrzewski, S Dapprich, A D Daniels, M C Strain, O Farkas, D K Malick, A D Rabuck, K Raghavachari, J B Foresman, J V Ortiz, Q Cui, A G Baboul, S Clifford, J Cioslowski, B B

- Stefanov, G Liu, A Liashenko, P Piskorz, I Komaromi, R L Martin, D J Fox, T Keith, M A Al-Laham, C Y Peng, A Nanayakkara, M Challacombe, P M W. Gill, B Johnson, W Chen, M W Wong, C Gonzalez, and J A Pople, *Gaussian 03, Revision B.05, Gaussian, Inc., Pittsburgh PA*, **2003**.
- [34] M Bisseyou, V Adohi-krou, R S P Zoakouma, R C A Yao-Kakou, N Ebby, *Acta Cryst.*, **2007**, E 63, 3987.
- [35] W J Hehre, I Radom, P. V. R Schleyer, A Pople, *Ab-Initio Molecular Orbital Theory*, J. Wiley-Interscience **1986**, New York.
- [36] J F Janak, *Phys. Rev.* **1978**, B18, 7165.
- [37] R Stowasser, R Hoffmann, *J. Am. Chem. Soc.* **1999**, 121, 3414.
- [38] R G Pearson, *Inorg. Chem.* **1988**, 27,734.
- [39] R G Pearson, *Proc. Natl. Acad. Sci. U.S.A* **1986**, 83, 8440.
- [40] V S Sastri, J R Perumareddi, *Corrosion*, **1997**, 53, 617.
- [41] P. M Niamien, D Sissouma, A Trokourey, A Yapi, K. H Aka, D Diabaté, *J. Soc. Ouest-Afr. Chim.* **2010**, 030, 49.
- [42] P M Niamien, H K Aka, A Trokourey, F K Essy, D Sissouma, Y Bokra, *ISRN Mat. Science* 2012, [CrossRef] <http://dx.doi.org/10.5402/2012/623754>.
- [43] P M Niamien, F K Essy, A Trokourey, A Yapi, H. K Aka, Diabaté, D. *Materials Chemistry and Physics* 2012, 136, 59.
- [44] J Fang, J Li, *Journal Mol. Struct. (THEOCHEM)* **2002**, 593,179.
- [45] I B Obot, N O Obi-Egbedi, S A Umoren, *Corros. Sci.* **2009**, 51, 276.
- [46] A. R. Leach, *Molecular modeling: principles and applications*, Prentice Hall, **2001**, Englewood Cliffs.
- [47] I Lukovits, A Shaban, E Kalman, *Russ. J. Electrochem.*, **2003**, 39,177